Chapter 5
Effect of Process Conditions on Fluidization

Abstract Previous chapters have illustrated the variety of fluidized-bed industrial applications and the importance of the process conditions on their operation. This chapter reviews experimental and theoretical studies on the influence of process conditions (temperature, pressure, presence of liquid, fines and fines size distribution) on the fluidization quality of gas-solid fluidized-bed reactors. The chapter begins with an overview of the effect of process conditions on fluidization highlighting the role of the hydrodynamic and interparticle forces on fluidized-bed behaviour. A brief review of the interparticle forces is reported to explain the foundation for the understanding of the factors responsible for the changes in fluidization at process conditions. Hence, the chapter discusses specifically the effect of temperature, pressure and other special conditions in the fluid bed, at minimum fluidization conditions, in the expanded fluid bed and at minimum bubbling conditions, showing how correlations and models established at ambient temperature and pressure may lead to misleading predictions at super- ambient conditions.

5.1 Introduction

A great deal of research has been carried out at ambient conditions with special attention being paid to evaluate the effect of physical properties of the particles on the enhancement of gas-solid contact and, as a consequence, chemical conversion; see Rowe et al. (1978) and Grace and Sun (1991). When we are considering the stability of a suspension, particle size and particle size distribution become important. For example, a suspension of 1 μm particles in air may remain stable for many minutes, whereas 100 μm particles will settle out in seconds. Similarly, flow rates of particles from hoppers, standpipes and most other aspects of particle behaviour depend on particle size. It is also known that addition of fine particles to a powder of coarser particles tends to improve its fluidization characteristics.

We dedicate this chapter to the late Dr. David Newton (formerly Head of the Fluidization Group at BP Chemicals Sunbury), a close colleague and friend, who contributed significantly to the work described herein.

It is on the basis of a variety of small scale tests developed at ambient temperature and pressure that fluid-dynamic models and correlations have been established and have been used for design criteria and performance predictions for fluid bed units working at high temperature and pressure. For a long time, the influence of the operative conditions on the fluid-dynamic characteristics of the system has been considered by simply accounting for the variations of the gas properties, namely its density and viscosity. However, extrapolating results and relationships from those developed at ambient conditions is reliable only when the hydrodynamic forces (HDFs) dominate the fluidization behaviour. Overlooking possible modifications induced by temperature and pressure to the structure of the fluidized bed, which can cause drastic changes in the fluidization behaviour and stability of the powders between ambient conditions and at high temperatures and pressures, is likely to lead to a misleading prediction of the fluid-bed performance and thus to errors in evaluating heat and mass transfer phenomena. A "reliable prediction" of the fluidization behaviour at unit operational conditions is of major importance, given that many of the industrial plants exploiting fluidization technology have been designed for operations run at thermal levels and pressure well above the ambient conditions, as described in the previous chapters.

Given the relevance of its applications, research on the influence of temperature and pressure on fluidization has been gaining interest, but findings are still controversial, as reported by Knowlton (1992) and Yates (1996) in their reviews on the subject. The positive effect of increased pressure in a fluidized bed is known to enhance bed-to-surface heat transfer coefficients in beds of Geldart Group A powders because of the suppression of bubbling, while in beds of Group B materials the enhancement is through an increase in the gas convective component of the transfer coefficient (see Sect. 5.3.3). Increased temperature can be responsible for modifications in the structure of fluidized beds causing in turn dramatic changes in the fluidization behaviour. A satisfactory understanding of the phenomena which are responsible for such changes has not yet been achieved. Much of the controversy still holds because the relative importance of the interparticle forces (IPFs) and hydrodynamic forces (HDFs) on the flow behaviour of the particles remains undefined.

Most of the disagreement on the relative role of HDFs and IPFs on the fluidizability of powders lies in the uncertain nature on the IPFs involved and in the difficulty of measuring them directly. Seville and Clift (1984) approached this problem introducing IPFs in a controlled manner and monitoring changes in the fluidization behaviour. Lettieri (1999) showed how the combined effect of temperature and presence of liquid can enhance the role of IPFs causing changes in the fluidization behaviour of industrial powders.

When trying to describe the fluidization of different materials the nature of the forces acting between adjacent particles becomes of major importance. It is well-known that finely divided Group C powders are very difficult to fluidize. The commonly accepted reason for this behaviour is the dominance of surface forces. The ratio of the surface forces to body forces increases with diminishing particle size. Hence, the fluidization of very fine materials, belonging to Group C is

dominated by the interparticle forces, which are greater than those transmitted to the particles by the fluidizing gas, Baerns (1966).

On the other hand interparticle forces are considered negligible when studying the fluidization behaviour of Group B and Group D powders. It is well established in the literature that interparticle forces also exist in Group A powders, although their importance as compared to body forces is not yet unequivocally defined. This is mainly due to the difficulty in recognizing the nature of the interparticle forces involved and, therefore, to quantify their effect on the fluidization behaviour.

The debate on the role of the IPFs and HDFs on the stability of Group A powders still divides into two groups the scientific world working on this matter. The physical origin of the stable behaviour of Group A powders has been studied theoretically, and two different approaches have been taken, one being based on the contention that bed stability is dominated by the hydrodynamic forces, see Foscolo and Gibilaro (1984), and the other that the interparticle forces are the controlling factor, see Mutsers and Rietema (1977). The physical origin of the stability of Group A powders has also been studied at an experimental level. Abrahamsen and Geldart (1980) and later Xie and Geldart (1995) investigated the stable behaviour of Group A materials by using a measurable parameter, the u_{mb}/u_{mf} ratio, which they defined as capable of predicting the aeratability of the powders. Xie and Geldart (1995) used the u_{mb}/u_{mf} ratio to correlate their experimental results obtained on the entire range of Group A materials, changing gas adsorption and operational conditions. They concluded that this parameter reflects both the effects of interparticle forces and hydrodynamic forces on the fluidization behaviour of fine powders. However, the usefulness of the u_{mb}/u_{mf} ratio as a discriminating test between low and high temperature was critically assessed by Newton et al. (1996) on the basis of experimental results obtained from fluidization at high temperature of some FCC catalysts.

Various other authors studied experimentally the stability of Group A powders with increasing temperature. Much debate on the interpretation of the results and the relative importance of the IPFs and HDFs is still in progress, mainly due to the difficulty of recognizing the nature of the interparticle forces involved and therefore of quantifying their effect on the fluidization behaviour. It is therefore necessary at this point to review the types and nature of the interparticle forces which might be encountered.

5.2 Interparticle Forces

Particle-particle contacting can be the result of different mechanisms of adhesion, the ones discussed in this chapter are shown in Table 5.1. An extensive review on the subject is reported in Israelachvili (1991).

Initially, the interparticle forces which arise without material bridge are discussed. A review on the capillary forces follows. Finally, the effect of temperature on the properties of the particle surface is discussed. A review on the formation of solid and sintered bridges is also presented.

Table 5.1 Mechanism of adhesion

Without material bridges	With material bridges
Van der Waals forces	Capillary forces
Electrostatic forces	Solid bridges
Magnetic forces	– Sintering
Hydrogen bonding	

5.2.1 Van Der Waals Forces

Electrostatic, capillary and van der Waals forces are said to be the most important to fluidized beds of fine powders. These forces depend on the particle size and the interparticle separation, usually becoming stronger with decreasing particle size and particle-particle separation. Other factors such as particle shape, surface roughness, gas humidity, moisture content and contamination also play a role. These factors can be affected by process conditions, for example high temperature.

Molecular or van der Waals forces arise from random motion of the electrons in the surface molecules. They are comprised of three types:

- Forces between polar molecules
- Forces between molecules polarised by fields of other molecules
- Forces of dispersion between non-polar molecules, due to the local polarization produced in molecules by the random fluctuation of electrons.

Intermolecular and interparticle forces are very different. The intermolecular forces decay with increasing molecular separation, z_o, as z_o^{-7}, whereas the interparticle forces as z_o^{-2}. In order to scale up the van der Waals forces to bodies having sizes larger than the molecular dimension, the Hamaker theory (Hamaker 1937) can be used. This assumes that the interaction energies between the isolated molecule and all the molecules in the large body are additive and non-interacting. Thus, the net energy can be found by integrating the molecular interactions over the entire body. The attraction force, F_a, for two perfectly spherical and rigid particles having diameters d_1 and d_2 at a separation distance a is:

$$F_a = \frac{AR}{12z_o^2} \tag{5.1}$$

where $R = d_1 d_2 / (d_1 + d_2)$, A is the Hamaker (materials-related) constant and z_o is the surface separation, which takes a minimum value of the order of the intermolecular spacing (generally assumed to be 4 Å). Values for the constant A can be found in Israelachvili (1991). The range of values for the Hamaker constant are quite small. For most solids interacting across vacuum or air A $\sim$ 4–40 $\times$ 10^{-20} J.

Rietema et al. (1993) calculated the minimum value for the parameter a taking into account a repulsive force as well as attractive and using a net force $F_{attractive}$-$F_{repulsive}$. In this way they evaluated a smaller value for the minimum surface separation of 2.23 Å. In the light of this calculation they estimated also the cohesion

force due to van der Waals forces for two perfectly spherical and rigid particles having diameters and density of a typical Group A material. This was several order of magnitude greater than the gravitational force. Rietema et al. (1993) also elaborated a fairly complicated model to account for particle deformation when evaluating the cohesive force between particles. Rietema and Piepers (1990) and Musters and Rietema (1977) interpreted the role of the van del Waals forces as the origin of the interparticle forces. They assumed that van del Waals forces are the controlling factor in the stable behaviour of group A powders, as opposed to the theory developed by Foscolo and Gibilaro (1987), already introduced in Chap. 1, according to which hydrodynamic forces dominate the transition from particulate to bubbling fluidization.

Massimilla and Donsi' (1976) also used Eq. 5.1 to calculate the van der Waals attractive forces between rigid particles. They used the following binomial formula to account for particle deformation:

$$F_a = \frac{A}{6a^2}\left(1 + \frac{A}{6\pi a^3 H}\right)R \qquad (5.2)$$

where H is the hardness of the softer of the bodies in contact, which they quoted to be 10^7 N/m^2 for FCC catalysts. The cohesion force increased by several hundred times when using Eq. 5.2. Massimilla and Donsi' (1976) stated that the second term in Eq. 5.2 is negligible for materials with hardness greater than 10^7 N/m^2.

The comparison between fluidization behaviour of Group A powders and the magnitude of the cohesive force obtained using Eq. (5.1) or (5.2), led Massimilla and Donsi' (1976) to investigate the particles' surface, in order to establish correct values for local radii of curvature R to enter into the equations. They observed the presence of surface asperities in the form of sub-particles, and were a common characteristic of all materials analyzed. Massimilla and Donsi' (1976) stated that such asperities become the sites at which contact takes place. Thus, the contact forces between solids are smaller by orders of magnitude according to the ratio between sub-particles diameter and particle size. By accounting for surface irregularities the cohesive force can be reduced by about two orders of magnitude. However, this still leaves the cohesive forces greater than the particle weight. Massimilla and Donsi' (1976) showed that for particles having diameters above 40 μm, the cohesive forces remain constant, while gravity forces increase with the cube of the particle diameter. This confirms the well-known reduction of the influence of the interparticle forces as the diameter of the particles increases.

In conclusion it can be said that whatever method is used it results in an overestimation of the attraction force between two particles, particularly if the deformation of the particles is accounted for. If the cohesive forces were this large the natural state of a Group A powder would be paste-like and it would never be fluidizable.

5.2.2 Electrostatic Forces

Particle adhesion due to static electricity is caused by the motion of electric charges on the surface of the particles at contact. This leads to the formation of an electric double layer surrounding the charged particles, in which positively charged elements prevail on one side and negatively charged ones on the other. Electrostatic forces depend on a number of variables difficult to evaluate, such as particle local geometry, surface roughness, presence of impurities, humidity and moisture in the molecular structure.

A fluidized bed is, by its very nature, a place where continuous contact and separation of solid particles occur, as well as the friction of the particles against others, and against the walls of the fluidized-bed container. Such circumstances should favour charge generation during fluidization, which may represent a potential safety hazard.

Boland and Geldart (1971) were amongst the first authors to contribute to the understanding of electrostatic charging in fluidized beds. They found that most of the particle-particle charging in the bed was associated with the passage of bubbles. They measured opposite sign voltages at the nose and wake regions of the bubbles, a phenomenon not entirely understood, but which led to the suggestion that a different mechanism of charge transfer takes place at the nose and wake region of the bubble. Frictional and kinetic effects may be more important in the wake region where particle motion is more intense, and consequently particle charging higher. It was also thought that a difference in voidage between the nose and the wake region could be the cause of the change in resistance, resulting in a different mechanism of charging. Electrostatic forces are difficult to control; however, by increasing the relative humidity of the fluidizing gas and the conductivity of the particles' surfaces it is possible to reduce the electrical resistance of the particles.

5.2.3 Magnetic Forces

A comprehensive survey on the effect of magnetic forces on fluidized beds was reported by Siegell (1989). Siegell reported that in the bubbling regime magnetic fields, with the smallest gradients along the height of the bed, produce a more uniform fluidization. Measurements of pressure fluctuations in the bed were greatly reduced with increasing magnetic field strength. More uniform porosity distribution in the bed was also reported as an effect of the bed magnetization, the latter causing though a decrease in the heat transfer coefficient. Given the stabilizing effect of magnetic fields, magnetized fluidized beds have been used to improve different industrial processes.

5.2.4 Capillary Forces

When a powder is in equilibrium with a dry atmosphere, at ambient conditions, the electrostatic or magnetic forces may be the only forces to consider at the contact point with another particle. If the humidity of the atmosphere is increased, then capillary forces may become an important component of the interparticle forces. At low humidity, capillary forces are caused by adsorption of water vapours on the surface of the particles. In this case the adhesion force between two particles depends on them coming close enough together for the adsorbed layers to overlap. As the relative humidity approaches saturation, then condensation occurs, causing the thickness of the adsorbed liquid layers to increase and generate more stable liquid bridges at the contact point between particles.

The mechanism of particle agglomeration due to liquid bridges has been widely studied given its importance in various industries. For example, it is beneficial in the process of granulation, which is extensively applied in pharmaceutical, mineral and fertilizer industries. However, it can also be deleterious causing serious problems in the handling of sticky particulate materials. In agglomeration processes the capillary forces can become so strong that fluidization can be lost completely, a phenomenon known as "wet quenching". On the other hand, the liquid bridges may subsequently evaporate, leaving the particles permanently agglomerated in solid bridges, and give place to a phenomenon called "dry quenching".

D'Amore et al. (1979) reported on the influence of moisture on the fluidization characteristics of non-porous and porous materials. They emphasized that particle porosity is the property which affects the ability of the materials to retain water without losing their fluidizability characteristics. Seville and Clift (1984) reported on the effect of liquid loading on the fluidization of Group B materials. They observed changes in the fluidization behaviour, which shifted through Group A to C, upon the increasing addition of liquids and the corresponding increase of the IPFs generated. Tardos et al. (1985) also studied the destabilization of fluidized beds due to agglomeration. They found that the limiting velocity at which the bed could be still fluidized was dependent on the amount of liquid added as well as the bed and fluid properties.

The approach taken to model the agglomeration process has been to scale up forces between pairs of particles to systems of multi-particles such as fluidized beds. Two different approaches have been developed to model the behaviour of wet agglomerates, one based on the assumption that the dynamic forces (dominated by viscosity) are the controlling factor, the other that the static forces (dominated by surface tension) are more important. Ennis et al. (1991) in their work on granulation phenomena between wet particles neglect static, consider that the energy loss during collision of two particles is due to the viscous dissipation in the liquid layer. They introduced a viscous Stokes number to predict the minimum velocity required for two coated spherical particles to rebound:

$$St^* = \frac{2\,m\,v_o}{3\,\pi\,\mu_l\,R^2} = \frac{8\,\rho\,v_o\,R}{9\mu_l} = \left(1 + \frac{1}{e}\right)\,\ln\left(\frac{2\,\delta}{3h_a}\right) \Rightarrow \left\{\frac{> 1\ \text{rebound}}{< 1\ \text{adhesion}}\right\} \quad (5.3)$$

where v_o is the velocity of particle collision, m and R are the particle mass and radius respectively, h_a is the height of the surface asperity, μ_l and δ are the viscosity and thickness of the liquid layer respectively, and e is the coefficient of restitution.

Simons et al. (1993) and Fairbrother (1999) considered the capillary static forces to derive a simple model capable of predicting the rupture energy of pendular liquid bridges, with only knowledge of the liquid volume employed to generate the liquid bridge itself:

$$W^* = k\,V_b^{*\,0.5} \quad (5.4)$$

where W^* is the dimensionless rupture energy ($W^* = W/\gamma\,R^2$, with γ the liquid surface tension), V^* is the dimensionless bridge volume ($V^* = V_b/R^3$) and k is a constant equal to 1.8. Their model predicts that the higher the gap value, the smaller the cohesive force between the particles.

Recently, Landi et al. (2011, 2012) validated the theories above in their investigation of the role of the interparticle forces on the flow behaviour of non-porous glass powders conditioned in a fluidized bed in controlled humid air at relative humidities between 13 and 98 %. Using the assumption that for non-porous materials, capillary condensation is the main phenomenon which is responsible for the formation of liquid bridges, they developed a model from shear experiments to predict the flow behaviour of the glass materials investigated and found that the tensile strength between the particles is a function of the cohesive force which, in turn, is a function of the bridge gap and of the asperity radius. In agreement with Simons et al. (1993) and Fairbrother (1999), the strength of the interparticle forces due to the capillary condensation between the asperities depended on the value of the capillary bridge gap.

5.2.5 Solid Bridges: Sintering

Temperature can have a considerable effect on particle adhesion if the contact between particles takes place at temperatures sufficiently high to cause softening of the particle surface and formation of interparticle bonds. The temperature at which softening occurs is called minimum sintering temperature, T_s. This is often lower than the fusion temperature of the bulk of the material.

The sintering process is characterised by the migration of particle material towards the bond zone. This can occur according to four different mechanisms, as described by Siegell (1984): surface diffusion, volume diffusion, viscous flow, vaporization. More than one mechanism can occur simultaneously depending on the material and on the conditions under which it is sintering. Transport of material

by diffusion and viscous flow are considered the most important in defluidization phenomena.

Sintering by diffusion involves the movement of individual atoms from high to low density regions and consequently migration of lattice vacancies from regions of high to low vacancy concentration. Diffusion can occur both at the surface, surface diffusion, and through the bulk of the material, volume diffusion. Sintering by surface diffusion usually happens in the early stages of all sintering processes, and is the cause of the initial adhesion between particles, which leads to the formation of agglomerates. Surface diffusion is followed by volume diffusion which causes the densification of the material. Sintering by diffusion is typical of crystalline and metallic materials.

The mass transfer mechanism in sintering by viscous flow is described, on a microscopic level, as due to the movement of entire planes of lattice, as opposed to the movement of single atoms which occurs in the diffusion mechanism. Thus, the rate of growth of the bond area is higher if sintering is by viscous flow, and the agglomerates which are formed are much more strongly bonded than those caused by a diffusion mechanism. This mechanism is the most important in defluidization because it is the most rapid.

When two particles of a fluidized bed come in contact with each other at high temperature they will tend to form a bond. Defluidization of a fluidized bed will take place when the bonds caused by sintering cannot be broken apart by the kinetic motion of the particles in the bed. Strong agglomerates, difficult to break, are caused by densification of the bond zone, which is not only a function of the temperature but also of how long the particles remain bonded. The strength of the agglomerates which form during defluidization depends also on the sintering mechanism. Siegell (1984) observed that friable agglomerates are formed during sintering by diffusion, and that this mechanism does not alter the original shape of the particles.

Compo et al. (1987) have used thermo-mechanical analysis (TMA) to quantify the sintering temperature; they correlated the dimensionless excess velocity (u − u_{mfs})/u_{mfs} with the dimensionless excess temperature (T − T_s)/T_s, where u_{mfs} is the minimum fluidization velocity at the minimum sintering temperature calculated from the value at ambient conditions using the Ergun equation. A theoretical model had been developed earlier by Tardos et al. (1985) to predict the limiting gas velocity U_s which is necessary to break the largest agglomerate in the bed and thereby to keep a bed of sticky particles continuously fluidized at temperatures above the minimum sintering temperature. The theoretical model was based on a force/stress balance on an agglomerate, cylindrical in shape and non-freely buoyant, which was assumed to occupy the entire cross-section area of the bed. The magnitude of the forces acting on the agglomerate, mainly due to the passage of bubbles, was estimated as a function of the excess fluidizing gas velocity, u − u_{mf}. The forces were then related to the pressure, q, acting on the agglomerate. Failure of the structure was predicted to occur when the pressure exceeded the maximum value q_{max} defined as:

$$q_{max} = \sigma_y \left(\frac{2h}{d_{ag}}\right)^2 A_1 \qquad (5.5)$$

where σ_y is the yield strength of the agglomerate, d_{ag} and h are the diameter and height of the agglomerate and A_1 is a coefficient approximately equal to 2.

An alternative approach was proposed by Ennis et al. (1991). Their model is based on the concept that, when particles collide, kinetic energy is dissipated via viscous losses in the fluid in the contact zone. At low collision velocities all energy is dissipated and the particles adhere. Above a certain critical velocity insufficient energy is dissipated in the fluid and the particles rebound.

Seville et al. (1998) described the phenomenon of defluidization caused by visco-plastic sintering. In a simple model of a fluidized bed, the particles are considered to remain in quiescent zones with relatively little movement until they are disturbed by the passage of bubbles. If the residence time in the quiescent zones is sufficiently long for the sinter necks to reach a critical size such that the agglomerates cannot be broken by the passage of the bubbles, then defluidization will start occurring. Seville et al. (1998) modelled the sintering phenomenon on the basis of a comparison of the characteristic residence time in which the particle motion is relatively small, t_{bb}, and the characteristic time necessary for the growth of sinter necks, t_s. The latter will change with temperature. In this approach, the time spent in the quiescent zone was assumed to be a function of the excess fluidizing velocity:

$$t_{bb} = \frac{K_1}{(u_{mfs} - u_{mf})} \qquad (5.6)$$

where K_1 is a constant which equals $2d_b/3$ when t_{bb} is considered the average time between the passage of bubbles, and d_b is the bubble diameter.

The critical time for sintering, t_s, sufficient to form an agglomerate which cannot be broken by the bubble was expressed as:

$$t_s = \left(\frac{x}{r}\right)^2 \frac{\eta}{k_1} \qquad (5.7)$$

where x is the neck radius at time t, r is the radius of the particle, η is the surface viscosity and k_1 is a factor dependent on both materials' properties and environmental conditions. Thus, Seville et al. (1998) obtained a quantitative relationship between the velocity required to keep the bed fluidized and bed temperature in terms of the surface viscosity of the particles by equating (5.6) and (5.7).

In order to predict the defluidization behaviour of a fluidized bed it is necessary to determine the initial sintering temperature of the particles. Like Compo et al. (1987), Lettieri (1999) measured the minimum sintering temperature of a range of materials using dilatometry analysis. Lettieri (1999) used thermomechanical analysis (TMA) to determine the expansion/contraction mechanisms taking place when
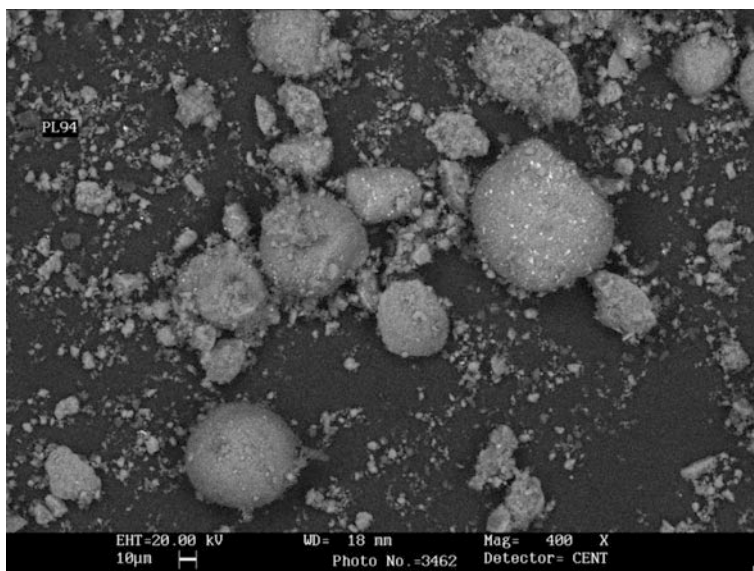
Fig. 5.1 SEM of an E-cat prior to high temperature fluidization (Lettieri 1999)

heating up samples of different industrial catalysts in order to relate changes in the materials' properties to their fluidization behaviour with increasing temperature. Figure 5.1 represents an SEM analysis of a sample of an equilibrium-catalyst (E-cat) prior to high temperature fluidization, showing a large number of fines stuck onto the surface of the larger particles. Figure 5.2, shows the effect of sintering after the powder was fluidized at high temperature, where strong bonds formed between the fine particles giving place to large agglomerates. The samples analyzed contained largely Si, Al, O and some C. Carbon was present on both the fines and the larger particles, but particles with lower levels of adhered fines appeared to contain less carbon.

The results of TMA carried out using a dilatometer are shown in Fig. 5.3, in which changes in the equilibrium catalyst dimension with increasing temperature are reported. Figure 5.3 shows an initial expansion up to 134 °C after which a sharp decrease in size occurs up to about 200 °C. The thermogram also shows a second very sharp shrinkage between 414 and 429 °C, after which the particle size remained constant until 900 °C, when a small amount of shrinkage takes place and which continued until the end of the experiment. A quantitative analysis of the TMA results showed a relative increase in size of 1.2 % occurred while heating the sample up to 132 °C. This was followed by a decrease in size of about 10 % between 132 and 250 °C. An even more important dimensional change occurred during the small temperature range between 414 and 429 °C where a relative size decrease of 11 % was quantified. Each shrinkage corresponds to sintering taking
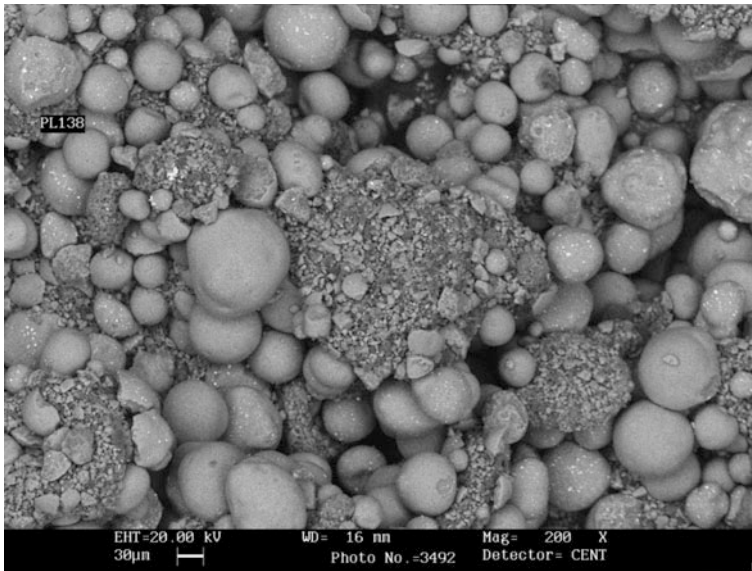
Fig. 5.2 SEM of an E-cat after high temperature fluidization (Lettieri 1999)
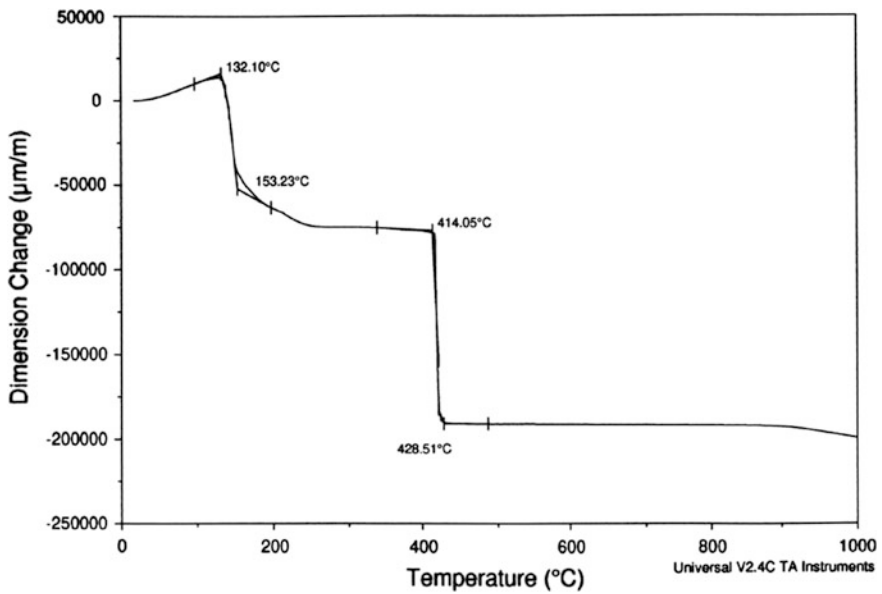

Fig. 5.3 TMA of an E-cat

place, in agreement with complete defluidization being observed between 150 and 200 °C (Lettieri 1999).

5.3 Effect of Temperature on Fluidization

The process conditions influence the operation of fluid-particle systems because they affect gas density and viscosity. Increasing temperature causes gas density to decrease and gas viscosity to increase. As mentioned before, most predictions of the fluidization behaviour at high temperatures have been based solely on considering such changes in the gas properties. However, this approach is valid under the condition that only hydrodynamic forces control the fluidization behaviour. Temperature can have a considerable effect on particle adhesion, enhancing the role of the IPFs on the fluidization quality, if the system is operated at temperatures close to the minimum sintering temperature of the particles, as discussed in Sect. 5.2.5. The effect of temperature on a fluidized bed is also strongly dependent on particle size, which in turn defines the type of particle-particle and fluid-particle interaction, thus determining the stronger or weaker role of the IPFs.

5.3.1 Effect of Temperature on Minimum Fluidization Conditions

The correlation most widely used to predict u_{mf} at ambient temperature is the Ergun equation, which is an expression for the pressure drop through a settled bed of solids:

$$(\rho_s - \rho_f)\, g\, (1 - \varepsilon_{mf})\, L = 150\ \frac{\mu\, L\, u_{mf}(1 - \varepsilon_{mf})^2}{(\phi\, d_p)^2\, \varepsilon_{mf}^3}\ + \ 1.75\frac{\rho_g\, L\, u_{mf}^2\, (1 - \varepsilon_{mf})}{\phi\, d_p\, \varepsilon_{mf}^3}\ \ (5.8)$$

In order to solve Eq. 5.8 the value of the bed voidage at minimum fluidization, ε_{mf}, and the sphericity of the particles, ϕ, need to be known a priori.

Wen and Yu (1966) showed that the voidage and shape factor functions in both the viscous and the inertial term of Eq. (5.8) can be approximated as:

$$\frac{1 - \varepsilon_{mf}}{\phi^2\, \varepsilon_{mf}^3} \approx 11; \qquad \frac{1}{\phi\, \varepsilon_{mf}^3} \approx 14 \qquad\qquad (5.9)$$

Combining Eqs. (5.8) and (5.9) Wen and Yu expressed the Ergun equation as follows:

$$Ga = 1650Re_{mf} + 24.5Re_{mf}^2 \qquad (5.10)$$

From the viscous term of Eq. (5.10) u_{mf} for small spherical particles (below about 100 μm) is given by:

$$u_{mf} = \frac{d_p^2(\rho_p - \rho_f)\,g}{1650\mu} \qquad (5.11)$$

For larger particles, it becomes:

$$u_{mf}^2 = \frac{d_p(\rho_p - \rho_f)\,g}{24.5\,\rho_f} \qquad (5.12)$$

Referring to any particle system belonging to any of the Geldart Groups, the qualitative effect of temperature on u_{mf} can be predicted from considerations on the gas density and viscosity terms in the Wen and Yu equation. For small particles, Eq. (5.11) shows that u_{mf} varies with $1/\mu$. Therefore, u_{mf} should decrease as temperature increases, when the viscous effects are dominant. Equation (5.12) predicts that u_{mf} will vary with $(1/\rho_f)^{0.5}$, thus u_{mf} should increase with temperature for large particles, when turbulent effects dominate. However, predictions with Eqs. (5.11) and (5.12) do not take into account possible changes in the voidage which may occur with increasing temperature. Various other correlations can be found in the literature to predict u_{mf} at high temperature, see Table 5.2.

Experimental verification of the temperature effect on u_{mf} has been reported by several authors. As predicted by the Wen and Yu equation, Botterill et al. (1982) observed a decrease of u_{mf} with increasing temperature for Group B materials, because of the consequent increase in gas viscosity, whereas for the large Group D powders they observed an increase in u_{mf}, because of the decrease of gas density, with the voidage at minimum fluidization being independent of temperature. The latter has been the subject of further experimental observations, Lucas et al. (1986), Raso et al. (1992), Formisani et al. (1998), and Lettieri et al. (2001a, b) all observed changes in the voidage at minimum fluidization with increasing temperature. Controversy is however reported on the phenomena which determine such changes. Lucas et al. (1986) explained changes in ε_{mf} with temperature on a hydrodynamic basis, suggesting a change in the flow pattern inside the bed. Contrary to this, Raso et al. (1992), Yamazaki et al. (1995), Formisani et al. (1998) and Lettieri et al. (2001a, b) related such changes to a variation of interparticle forces with increasing temperature. In particular, Formisani et al. (1998) investigated various Group A, B and D powders and observed a linear increase of the voidage of the fixed bed with temperature and a corresponding linear increase of ε_{mf} (Fig. 5.4) with a close similarity between the slope of the fixed bed voidage and the voidage at minimum fluidization. In line with the theory previously advanced by Rietema, they attributed the increase of the fixed bed voidage by assuming that the interparticle forces between cohering particles give rise to a powder structure with a certain mechanical

Table 5.2 Selected equations for the calculation of the minimum fluidization velocity, u_{mf}

| Authors	Equation	
Ergun (1952)	$150\dfrac{\mu_g u_{mf}}{(\phi d_p)^2}\dfrac{(1-\varepsilon_{mf})}{\varepsilon_{mf}^3} + 1.75\dfrac{\rho_g u_{mf}^2}{\phi d_p}\dfrac{1}{\varepsilon_{mf}^3} = g(\rho_p - \rho_g)$	
Carman (1937)	$u_{mf} = \dfrac{(\phi d_p)^2}{180}\dfrac{(\rho_p - \rho_g)}{\mu_g} g\left(\dfrac{\varepsilon_{mf}^3}{1-\varepsilon_{mf}}\right)$	
Miller and Logwinuk (1951)	$u_{mf} = \dfrac{1.25\times10^{-3}d_p^2(\rho_p-\rho_g)^{0.9}\rho_g^{0.1}g}{\mu_g}$	
Leva et al. (1956)	$u_{mf} = \dfrac{7.39 d_p^{1.82}(\rho_p-\rho_g)^{0.94}}{\rho_g^{0.06}}$	
Goroshko et al. (1958)	$u_{mf} = \dfrac{\mu_g}{\rho_g d_p}\left(\dfrac{Ar}{1400+5.2\sqrt{Ar}}\right)$	
Leva (1959)	$u_{mf} = \dfrac{8.1\times10^{-3}d_p^2(\rho_p-\rho_g)g}{\mu_g}$	
Broadhurst and Becker (1975)	$u_{mf} = \dfrac{\mu_g}{\rho_g d_p}\left(\dfrac{Ar}{2.42\times10^5 Ar^{0.85}\left(\frac{\rho_p}{\rho_g}\right)^{0.13} + 37.7}\right)^{0.5}$	
Riba et al. (1978)	$u_{mf} = \dfrac{\mu_g}{\rho_g d_p}\left(1.54\times10^{-2}\left(\dfrac{d_p^3\rho_g^2 g}{\mu_g^2}\right)^{0.66}\left(\dfrac{\rho_p-\rho_g}{\rho_g}\right)^{0.7}\right)$	
Doichev and Akhmakov (1979)	$u_{mf} = \dfrac{\mu_g}{\rho_g d_p}(1.08\times10^{-3}Ar^{0.947})$	
Wu and Baeyens (1991)	$u_{mf} = \dfrac{\mu_g}{\rho_g d_p}\left(7.33\times10^{-5}\times10^{\sqrt{8.24\log_{10}Ar-8.81}}\right)$	
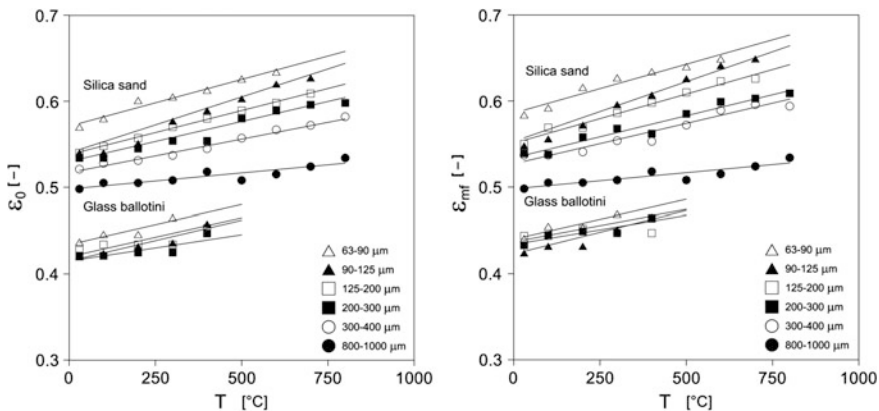
Fig. 5.4 Effect of temperature on the fixed bed voidage and minimum fluidization velocity for glass ballotini and silica sand particles of different size, Formisani et al. (1998)

strength in the packed bed and in turn in the bed at incipient fluidization and in the expanded state of homogeneous fluidization.

Lettieri (1999) reported on the effect of temperature on the minimum fluidization velocity of fresh industrial catalysts and catalysts doped with potassium acetate. The variation of minimum fluidization velocity with temperature was found to be

Fig. 5.5 Effect of temperature on the minimum fluidization velocity for an industrial catalyst doped with different levels of potassium acetate
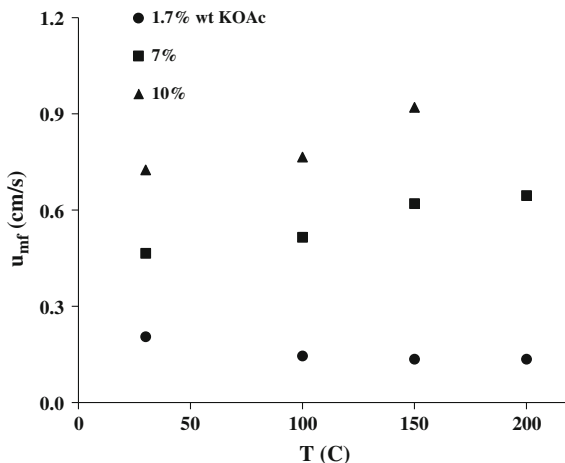
sensitive to whether the HDFs or IPFs dominated the fluidization behaviour. For all fresh catalysts, values of the minimum fluidization velocity were predicted by the viscous dominated term of the Ergun equation, once appropriate values for the sphericity factor and ε_{mf} were used. However, u_{mf} values obtained for the doped catalysts increased as a function of temperature, and the values for u_{mf} were found to deviate from the predictions with the Ergun equation due to a stronger role of the IPFs. Figure 5.5 shows the minimum fluidization velocity of the three doped silica catalysts as a function of temperature. u_{mf} decreased slightly with increasing temperature, when the catalyst was doped with only 1.7 %wt of potassium acetate. Values of u_{mf} obtained for the sample with 7 %wt remained fairly constant up to 100 °C, then increased slightly between 100 and 200 °C. A greater increase of u_{mf} as temperature increased was found for the sample doped with 10 %wt of potassium acetate.

More recently, several authors have investigated also the combined effects of temperature and particle size and particle size distribution (PSD) on minimum fluidization velocity, Lin et al. (2002), Bruni et al. (2006), Subramani et al. (2007), Hartman et al. (2007), Goo et al. (2010), Chen et al. (2010) and Jiliang et al. (2013). General observations demonstrated that that operating temperature and particle size distribution can influence the minimum fluidization velocity simultaneously, making variations of u_{mf} non-monotonic with temperature. Several correlations have been derived for the prediction of the minimum fluidization conditions at high temperature, these are however case specific. The debate of the phenomena causing changes in behavior with increasing temperature remains controversial with still much disagreement on the role of the hydrodynamic and interparticle forces.

5.3.2   *Effect of Temperature on Fluid-Bed Expansion and Richardson-Zaki Relationship*

As mentioned earlier, Group A particles are those which exhibit a region of uniform expansion for gas velocities above minimum fluidization. The non-bubbling expansion is characterized by the Richardson-Zaki (1954) equation (Chap. 1, Eq. 1.1), which was first used to correlate the homogeneous expansion of liquid fluidized beds. Bed expansion experiments in gas-solid fluidized beds were conducted by Godard and Richardson (1968) on various materials, characterized by a very narrow size distribution, and fluidized with air at pressures between 1 and 14 atm. They found that the relationship between the fluidizing velocity u and bed voidage ε could be expressed in the form of Eq. (1.1):

$$U/U_t = \varepsilon^n \tag{1.1}$$

The applicability of Eq. (1.1) to describe the bed expansion of Group A powders may suggest that the expansion mechanism of gas fluidized beds and liquid fluidized beds is similar. However, the validity of this comparison has not always been accepted. Massimilla et al. (1972) and Donsi' and Massimilla (1973) made some observations of the bubble free expansion of gas fluidized beds of fine particles and described the mechanism of bed expansion as due to nucleation and growth of cavities whose size ranges in the order of few particle diameters. At the same time, they also postulated that particles surrounding the cavities maintain the surface contacts, which is essential for the stability of the structure. They stated that the cavity growth mechanism of bed expansion probably occurs because of a broad distribution of interparticle forces.

This was evidenced by the different values of n found when comparing liquid fluidized beds and gas-solid systems. If for liquid systems, values of n were found to be equal to 4.8 in the viscous flow regime and 2.4 in the inertial regime, the values of the index n for powders were found to be higher than those predicted for uniform spheres fluidized by a liquid.

Various authors found that experimental values of n (indicated as n*) extrapolated from expansion profiles are greater than those predicted by the Richardson-Zaki correlations. Some of the data reported in the literature are shown in Fig. 5.6.

Godard and Richardson (1968) found values of n* between 4.7 and 8.9 for various materials fluidized with air at ambient conditions, the highest values were obtained for some phenolic resins. Massimilla et al. (1972) found values between 5.4 and 7, where the highest values were obtained for the finer and non-sieved materials. Geldart and Wong (1984, 1985) fluidized a wide range of powders at ambient conditions using various gases, such as air, argon, nitrogen and Arcton-12, and found values of n between 4 and 60, where the discrepancy becomes increasingly larger for those materials which showed higher degrees of cohesiveness. Similar results were also reported by Avidan and Yerushalmi (1982). Foscolo et al. (1987) reported values of n* close to the predicted ones for particles having a

Fig. 5.6 Comparison between experimental n* values obtained by various authors, at ambient conditions using different gases, with calculated n values using Richardson-Zaki correlations, Eq. (1.1)
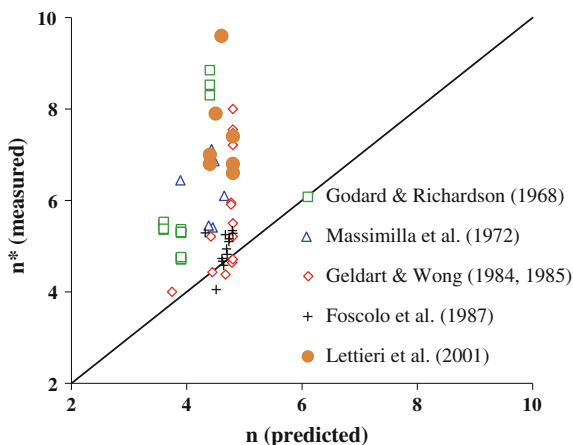
very narrow particle size distribution and fluidized with air, argon and CO_2. This was in agreement with the findings of Lettieri et al. (2001a, b) who investigated the effect of temperature on the expansion profiles of four FCC powders. Experimental values of n^* and u_t^* were determined from the expansion profiles plotted in the Richardson-Zaki form and found to be greater than those predicted, with values being within the range 6.4–9.6.

The discrepancy concerning u_t^* might be partly explained by the large extrapolation in the data that must be employed, i.e. from $\varepsilon = 0.6$ to $\varepsilon = 1$. However, Avidan and Yerushalmi (1982) stressed the great influence that the particle size distribution may have on the values obtained for u_t^*. They found lower u_t^* values for those catalysts characterized by a higher content of fines. This was in agreement with the results by Lettieri et al. (2000), where values obtained for the FCC3, which contained about 25 % of fines, were lower than those obtained for the other FCC catalysts containing respectively 5 and 16 % of fines.

Furthermore, it is important to mention that it is difficult to know which mean particle diameter to use when calculating u_t for powders with a wide particle size distribution. In fluidization, the surface-volume ratio, d_{SV}, is generally accepted as the most appropriate estimate of the mean particle diameter. However, if other possible geometrical diameters are considered, such as the surface average and volume average, d_S and d_V respectively:

$$d_S = \sqrt{\sum x_i d_i^2} \qquad d_V = \sqrt[3]{\sum x_i d_i^3} \tag{5.13}$$

where x_i is the mass fraction of particles in each size range given by the sieve aperture d_i, then the mean particle diameters for the three samples of fresh FCC catalysts calculated as d_{SV}, d_S and d_V are reported in Table 5.3.

Lettieri (1999) calculated the particle terminal fall velocity corresponding to the diameters in Table 5.3 for three FCC catalysts, and compared such values against

Table 5.3 Mean particle diameters

	d_{SV} (μm)	d_S (μm)	d_V (μm)
FCC 1	71	91	102
FCC 2	57	104	124
FCC 3	49	80	91

those obtained experimentally, and found that the values of u_t^* extrapolated at temperatures above 100 °C were of the same order of magnitude as u_{tS} and u_{tV}. For all FCC catalysts, u_t^* values obtained between 20 and 100 °C corresponded to a mean particle diameter much greater than either d_S or d_V.

Also Valverde et al. (2001) investigated the role of the interparticle forces on the homogenous fluidization and settling of fine powders. They proposed an extension of the Richardson-Zaki empirical correlation to predict the effect of the interparticle forces on the settling of fine powders in the presence of aggregates. Valverde et al. (2003) extended the previous study investigating the transition between the solid-like, fluid-like, and bubbling fluidization of gas-fluidized fine powders. Using optical probe measurements, they showed that the transition between the solid-like and the fluid-like regimes takes place along an interval of gas velocities in which transient active regions alternate with transient solid networks, making the prediction of the transition between the different regimes a complex task. Castellanos (2005) later studied the onset of fluidization of fine and ultrafine powders and attributed to the presence of clusters the observation of a highly expanded state of uniform fluid-like fluidization. Valverde and Castellanos (2008) combined the observations reported above proposing an extension of the Geldart classification of powders to predict the behavior of gas-fluidized cohesive particles taking into account interparticle forces. In the new diagram proposed by Valverde and Castellanos, the boundaries between the different types of fluidization are not defined solely by hydrodynamic and physical parameters such as fluid viscosity and particle density but are also a function of the fractal dimension of the agglomerates and the powder's compaction history.

5.3.3 Effect of Temperature on the Stability of Group A Powders

The transition from homogenous to bubbling fluidization can be predicted using the stability criterion developed by Foscolo and Gibilaro (1984), previously introduced in Chap. 1. We summarize here the fundamental assumptions of the model:

- hydrodynamic forces, i.e. gravitational force, buoyancy and drag force, control the stability of Group A powders, at both ambient and high temperatures.
- the buoyancy force, W_b, exerted on a particle is defined as a function of the density of the suspension, rather than of the fluid alone.
- the Richardson-Zaki equation is used to describe the relation between the velocity and voidage, with values of n = 4.8 for the viscous regime.
- by applying Richardson-Zaki equation, the pressure drop is expressed as $\Delta P \propto \varepsilon^{-4.8}$, and the drag force is given by $F_d \propto \varepsilon \Delta P \propto \varepsilon^{-3.8}$.
- Wallis' stability theory is applied to determine the transition between particulate and bubbling regime, determined as ε_{mb}.

The expression of the criterion was given in Chap. 1, Sect. 1.2.5, we write it again for convenience:

$$\left[\frac{g\,d_p(\rho_p-\rho_f)}{u_t^2\,\rho_p}\right]^{0.5} - 0.56\,n\,(1-\varepsilon_{mb})^{0.5}\,\varepsilon_{mb}^{n-1} = \left\{\frac{\text{positive, stable}}{\text{negative, unstable}}\right\} \qquad (5.14)$$

The Foscolo-Gibilaro model was developed for systems of spherical mono-sized particles, for which the values of n and u_t can be adequately predicted by the Richardson-Zaki correlations and the Stokes law, based on the surface-volume diameter.

Lettieri et al. (2001a, b) validated Eq. (5.14) for different FCC catalysts fluidized at high temperature and found that prediction of ε_{mb} didn't match with the experimental evidence, as the stability criterion predicted a much greater increase in the voidage at minimum bubbling than observed. In the original Foscolo-Gibilaro stability criterion, the constitutive equation for the interaction force on a single particle is expressed as the sum of the contribution given by the buoyancy force and by the drag force. The latter determines the homogeneous expansion of the bed, through its relation with n and u_t. Thus, given the discrepancy between the experimental n^* and u_t^* values shown in Figs. 5.6 and 5.7, Lettieri et al. (2001a, b) proposed a generalization of the stability criterion by re-formulating the drag force by imposing a general value n for the Richardson-Zaki index in the expression of the drag. Hence they obtain a generalized stability criterion that can be expressed as follows:

$$\left[\frac{2\,g\,d_p\,(\rho_p-\rho_f)}{3\,u_t^2\,\rho_p}\right]^{0.5} - n^{0.5}\,(1-\varepsilon_{mb})^{0.5}\varepsilon_{mb}^{n-1} = \left\{\frac{\text{positive, stable}}{\text{negative, unstable}}\right\} \qquad (5.15)$$

The generalized model, Eq. (5.15), allows to use values of n and u_t which can be different from those originally proposed. A comparison between predictions obtained from the original and generalized Foscolo-Gibilaro model for three fresh FCC, from 20 to 650 °C are reported in Fig. 5.7. These results demonstrate clearly the importance of using a relation between the drag force and the expansion parameters which correctly describes the characteristics of the homogeneous fluid-bed system. When n^* and u_t^* values, that characterize the bed expansion, are

Fig. 5.7 Experimental u_t^* values *versus* calculated values of u_{tV} and u_{tS} for three fresh FCC catalysts, from 100 to 650 °C (Lettieri 1999)
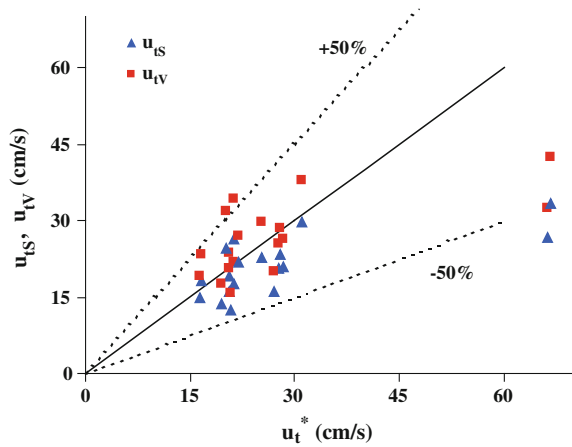
Fig. 5.8 Comparison between predictions obtained from the original and generalized Foscolo-Gibilaro model for three fresh FCC, from 20 to 650 °C (Lettieri 1999)
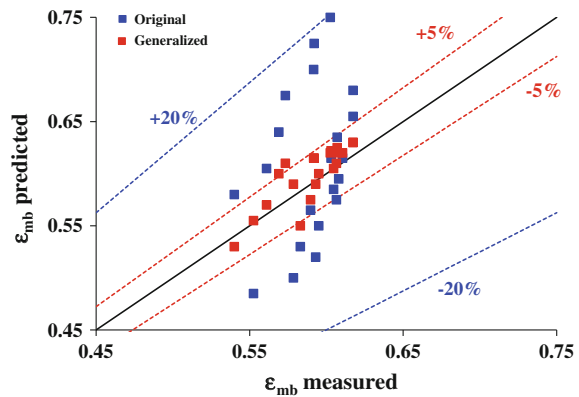
introduced in the Foscolo-Gibilaro model, this is capable of predicting the transition between the particulate and bubbling regime with a smaller margin of error (i.e. ± 5 %), than the original model (i.e. ± 20 %) (Fig. 5.8).

5.3.4 Effect of Temperature on the Non-bubbling Ratio

The non-bubbling ratio, u_{mb}/u_{mf}, is reported to be one of the key parameters which characterizes the fluidization of fine materials. It is used as a measure of how fluidized beds expand or contract; the larger the u_{mb}/u_{mf} ratio the smoother the fluidization quality, and the better the aeratability of the materials. Abrahamsen and Geldart (1980) related the hydrodynamic properties of fluidized beds to the non-bubbling ratio. They performed measurements of the u_{mb}/u_{mf} ratio over a wide range of materials at ambient conditions using different gases. They proposed a

correlation to predict the non-bubbling ratio from the properties of the powder, i.e. particle diameter and fines content, and from the properties of the fluidizing gas, i.e. density and viscosity.

$$\frac{u_{mb}}{u_{mf}} = \frac{2300 \, \rho_g^{0.126} \, \mu^{0.523} \, \exp \, (0.716 \, F_{45})}{g^{0.934} \, (\rho_p - \rho_g)^{0.934} \, d_p^{0.8}} \tag{5.16}$$

According to the Abrahamsen and Geldart (1980) correlation, u_{mb}/u_{mf} varies as a function of the properties of the powder when the gas properties are not changed. For example, an increase in the fines contents due to attrition, will cause u_{mb}/u_{mf} to increase and the fluidization quality to improve. However, if the fines content increases too much, the fluidization behaviour could eventually shift from Group A type to cohesive Group C. Conversely loss of fines, which may occur through mal-functioning of a cyclone, reduces u_{mb}/u_{mf}. When u_{mb}/u_{mf} becomes close to 1, the flow behaviour can shift from a Group A into a Group B type fluidization.

The Abrahamsen and Geldart (1980) correlation predicts the effect of operating conditions on fluidization quality through changes in the gas density and viscosity terms ($u_{mb}/u_{mf} \sim \mu^{0.523} \cdot \rho^{0.126}$), assuming that only HDFs are present. As temperature increases, changes in the viscosity term dominate, and the correlation predicts that u_{mb}/u_{mf} should increase, thus improving the fluidization quality.

Newton et al. (1996) reported on the effect of temperature on the u_{mb}/u_{mf} ratio of some fresh FCC catalysts, which were fluidized in a 100 mm i.d. vessel from ambient conditions up to 500 °C. They observed a decrease of the u_{mb}/u_{mf} ratio with increasing temperature for all FCC catalysts. The experimental values were compared with the predictions given by the Abrahamsen and Geldart (1980) correlation. Experimental trends were found to be opposite to the predicted ones. Furthermore, Newton et al. (1996) observed that differences existing between the catalysts at ambient conditions, in terms of the u_{mb}/u_{mf} ratio, disappeared at high temperature, altering the ranking order of the powders.

Xie and Geldart (1995) proposed Eq. (5.17), a slightly modified version of Eq. (5.16), which was developed on the basis of tests carried out also at high temperature:

$$\frac{u_{mb}}{u_{mf}} = \frac{333 \, \rho_g^{0.19} \, \mu_g^{0.37} \exp \, (0.716 \, F_{45})}{g^{0.934} \, (\rho_p - \rho_g)^{0.934} \, d_p^{0.8}} \tag{5.17}$$

They also proposed a further version, Eq. (5.18) which was obtained by considering that u_{mb} changes with temperature are proportional to $\rho_g^{0.13} / \mu^{0.5}$, as shown in Eq. (5.15):

$$u_{mb} = 0.3 \exp \, (0.716 \, F_{45}) \frac{d_p \, \rho_g^{0.13}}{\mu^{0.5}} \tag{5.18}$$

and that u_{mf} is inversely proportional to μ, see Ergun (Table 5.2). Then, by taking gas density as inversely proportional to absolute temperature, and gas viscosity as proportional to the square root of absolute temperature, changes in u_{mb}/u_{mf} were expressed as proportional to $T^{0.12}$, and the following correlation was proposed:

$$\left(\frac{u_{mb}}{u_{mf}}\right)_T = \left(\frac{u_{mb}}{u_{mf}}\right)_{297} \left(\frac{T}{297}\right)^{0.12} \tag{5.19}$$

Note that an experimental value of the non-bubbling ratio at ambient temperature is required in this equation.

As temperature increases the gas density decreases whilst gas viscosity increases. It is therefore predicted that both u_{mf} and u_{mb} should decrease, with u_{mf} decreasing faster than u_{mb} with increasing temperature. Thus, Eq. (5.19) predicts that the u_{mb}/u_{mf} ratio should increase. Lettieri (1999) tested all three equations: Eqs. (5.16), (5.17) and (5.19) for three FCC catalysts, and found that Eq. (5.16) predicted a much greater increase of the non-bubbling ratio than the one found experimentally. Thus, extrapolating the effect of temperature on the fluidization of these catalysts from Eq. (5.16), may lead to a misleading prediction of the non-bubbling ratio at high temperature. On increasing temperature, Eq. (5.19) gave a better prediction of u_{mb}/u_{mf} values for two of the FCC catalysts with increasing temperatures. On the whole, all of the equations gave predictions with a scatter of ± 30 %, as shown in Fig. 5.9.

More recently, Girimonte and Formisani (2009) investigated the influence of operating temperature on the transition to the bubbling regime for some FCC, silica and corundum sands, at temperatures ranging from 30 to 500 °C. They determined the minimum bubbling velocity using four different methods and showed that depending on the method adopted, different results can be obtained for u_{mb} with increasing temperature. The first method relied on the classical direct observation of the velocity at which the first bubble erupted on the free surface of the bed. The second method was based on the measurement of the pressure drop across the

Fig. 5.9 Non-bubbling ratio, experimental *versus* predicted values for three FCC catalysts from 20 to 650 °C (Lettieri 1999)
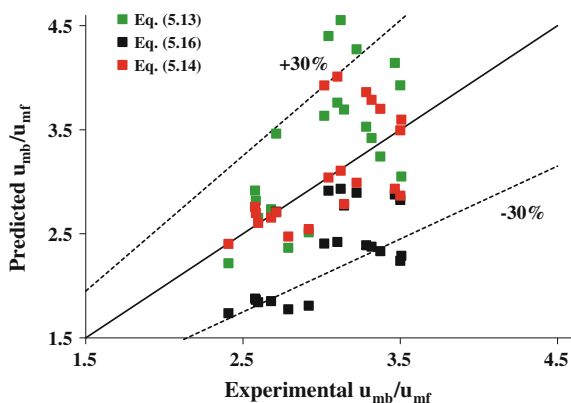
whole bed, and u_{mb} was taken at the point where a shallow minimum of the Δp versus u curve occurs. The last two methods were derived from the analysis of the "fluidization map", namely the examination of the expansion behaviour of the bed over a range of fluidization velocities from the fixed bed state to the bubbling regime. Based on the experimental evidence, Girimonte and Formisani (2009) concluded that the visual observation of the bed and the method based on the detection of the pressure drop minimum were unreliable for correctly determining the starting point of bubbling. They concluded that the analysis of bed expansion as a function of the fluidization velocity is the only method allowing the reconstruction of the succession of phenomena through which a stable flow of bubbles across the solid mass ensues.

Girimonte and Formisani (2014) reported in further experiments on the effect of temperature on the fluidization of FCC particles. They used a combination of non-invasive optical technique for acquiring images of bubbles' eruption at the free surface and results from bed collapse tests to determine the transition to bubbling fluidization with increasing temperature. Their experiments showed that high temperature influences the quality of bubbles producing a smoother regime of bubbling, which they attributed to the thermal enhancement of IPFs that leads to higher porosity and lower interstitial flow in the emulsion phase.

In summary, high temperature clearly affects the stability of fluidized beds of Group A powders; well established theories and models fail to predict correctly the voidage at minimum bubbling with increasing temperature. Models corrected on the basis of experimental data are capable to reproduce correct trends; however a priori predictions of the fluid bed stability with increasing temperature are yet to be achieved. The challenge here still is in the ability to describe the forces that determine the transition from particulate to bubbling fluidization. Hence, some kind of quantification of the effects of the IPFs on fluidization is needed in order to advance the understanding of fluidization at high temperature.

5.4 Pressure

A number of fluidized-bed processes are operated at elevated pressures, gasification and polymerization being two examples. It is therefore important to know how fluidized beds behave under these conditions and how this behaviour differs from that observed at ambient pressure. Important to consider are the properties of beds over the full range of gas velocities from minimum fluidization through the bubbling regime to turbulent flow and velocities at which particle elutriation occurs. The effect of pressure on jet penetration length from immersed orifices and bed-to-surface heat transfer is also crucial for design and is discussed in what follows.

Fig. 5.10 Effect of pressure on U_{mf} based on Eq. 5.20 (Based on Rowe 1984)
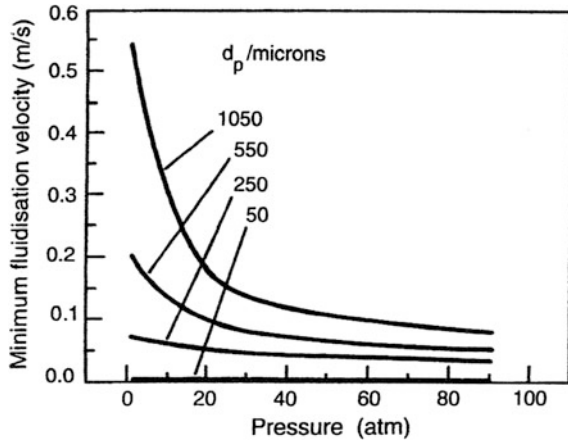
5.4.1   Minimum Fluidization Velocity

The effect of pressure on U_{mf} may be estimated qualitatively by rearranging the Ergun equation as follows:

$$U_{mf} = \frac{\mu}{\rho_f d_p} 42.9 \left(1 - \varepsilon_{mf}\right) \left\{ \left[1 + 3.0 \times 10^{-4} \frac{\varepsilon_{mf}^3}{\left(1 - \varepsilon_{mf}\right)^2} Ar \right]^{1/2} - 1 \right\} \qquad (5.20)$$

Rowe (1984) applied Eq. 5.20 to particles of density 1250 kg/m^3, a range of sizes and a value of ε_{mf} of 0.5 (Fig. 5.10).

It is clear that for particles with diameters less than 100 μm (Group A) pressure is predicted to have little effect, the reason being that gas flow around these small particles is laminar and the fluid-particle interaction force is dominated by gas viscosity which is largely independent of pressure in the range considered. With increasing particle size inertial forces become more important and at $d_p > 500$ μm (Group B) they begin to dominate over the viscous forces causing U_{mf} to decrease sharply with pressure up to about 20 bar and more gradually thereafter. King and Harrison (1982) also showed that U_{mf} is independent of pressure for laminar flow ($Re_{mf} < 0.5$) while for turbulent flow ($Re_{mf} > 500$) it is inversely proportional to the square root of gas density and hence pressure. Similar conclusions were reached by Olowson and Almstedt (1991) who measured U_{mf} for a range of particles in Groups B and D at pressures from 0.1 to 0.6 MPa and found a general decrease with increasing pressure.

5.4.2   Bubble Dynamics

A great deal of work has been carried out on the effect of pressure on bubbling beds much of which was summarised by Yates (1996) and subsequently (Yates 2003).

As in the case of minimum fluidization velocity the behaviour is a function of the type of bed material divided amongst the four Geldart groups.

5.4.2.1   Group A Materials

It is generally agreed that while U_{mf} is unaffected the region of bubble-free bed expansion between U_{mf} and U_{mb} increases with increasing pressure. In addition at the same values of volumetric gas flow rate bubbles in beds of Group A materials become smaller as pressure increases. There could be two reasons for this: (a) a greater proportion of gas flows through the emulsion phase as a result of an increase in emulsion-phase voidage; (b) the stability of bubbles decreases causing them to break up into smaller voids. The question of bubble stability has been considered since the early days of fluidization and two models have emerged from these studies. In the theory of Davidson and Harrison (1963) it was assumed that as the bubble rises the shear force exerted by the particles moving down relative to the bubble sets up a circulation of gas within the void with a velocity u_c which approximates to the bubble rise velocity u_b. When, through coalescence, the bubbles grow in size and their velocity increases a point is reached where u_c exceeds the terminal fall velocity, u_t, of the particles within the bubble and solids in the wake will be drawn up causing the bubble to break into smaller units with lower rise velocities. Bubbles would therefore be expected to reach a limiting size determined by u_t and beds of Group A particles should show "smoother" fluidization than beds of coarser, denser materials and since values of u_t decrease with increasing pressure (Haider and Levenspiel 1989) this behaviour should increase with pressure, an effect widely reported in the literature (Yates 1996).

An alternative theory proposes that bubble break-up is caused by a Taylor instability in the bubble roof allowing particles to rain down through the void and divide it in two (Clift et al. 1974). A factor determining the stability of the bubble roof is taken to be the apparent kinematic viscosity of the emulsion phase so that bubbles become more unstable as this viscosity decreases a change which would result from an increase in emulsion-phase voidage a trend already noted to occur with increasing pressure. An X-ray study by King and Harrison (1980) of beds of particles in Groups A and B at pressures of up to 25 bar showed that both bubbles and slugs broke up by fingers of particles falling in from the roof an effect that became more pronounced with increasing pressure.

5.4.2.2   Group B Materials

King and Harrison (1980) found bubble size to be independent of pressure up to 25 bar but Hoffmann and Yates (1986), also using X-rays, found mean bubble diameters to increase slightly up to 16 bar and to decrease thereafter up to 60 bar. This work also showed an increase in bubble coalescence as pressure was increased but that their stability was lower at higher pressures causing them to break up into

ever smaller units; at the highest pressures studied bubbles were hard to identify at all the bed having taken on the appearance of an ill-defined foaming mass of fluidized material. These results were later confirmed in a study by Olowson and Almstedt (1990).

5.4.2.3 Group D Materials

These have been little studied relative to those in Groups A and B. King and Harrison (1980) studied spouted beds of 1.1 mm diameter glass spheres at pressures of up to 20 bar and found a marked decrease in minimum spouting velocity with increasing pressure and concluded that Group D materials should follow the same trends as those shown by Group B powders but at higher pressures.

5.4.3 Jet Penetration

When gas first enters a fluidized bed from an orifice in a supporting grid it does so either in the form of discrete bubbles or as a flame-like jet that decays into a stream of bubbles at some height above the grid. Whether jets or bubbles form was explored by Grace and Lim (1987) who, on the basis of much experimental evidence concluded that jets would form for values of the ratio:

$$\frac{d_{or}}{d_p} \leq 25.4 \tag{5.21}$$

where d_{or} and d_p are the diameters of the orifice and bed particles respectively. Under all other conditions bubbles rather than jets would form Hirsan et al. (1980) measured maximum jet penetration lengths, L_{max}, in beds of Group B materials up to pressures of 50 bar and found:

$$\frac{L_{max}}{d_p} = 26.6 \left(\frac{\rho_f}{\rho_p} \right)^{0.67} \left(\frac{U_0^2}{gd_p} \right)^{0.34} \left(\frac{U}{U_{cf}} \right)^{-0.24} \tag{5.22}$$

where U_0 is the orifice gas velocity and U_{cf} is the superficial velocity necessary to fluidize the polydispersed powder. The correlation shows that jet penetration length increases with pressure but decreases as the velocity of the fluidizing gas increases. Other similar correlations have been obtained by Yang (1981) and Yates et al. (1986).

5.4.4 Entrainment and Elutriation

Entrainment occurs when gas bubbles burst at the bed surface and throw particles into the freeboard space. At low gas velocities these particles fall back to the bed surface and are retained but as fluidizing velocity increases more particles are transported to ever greater heights giving rise to a particle-density gradient above the surface. For sufficiently tall freeboards there will be a height at which the density gradient falls to zero and above this height the entrainment flux will be constant. This height is called the transport disengaging height or TDH. At sufficiently high gas velocities particles will be carried out of the bed completely or elutriated. Elutriation is considered to be a first-order process such that the rate of elutriation of particles within a size range d_{pi} is directly proportional to the mass fraction of that size range x_i in the bed. Thus:

$$-\frac{1}{A_t}\frac{\mathrm{d}}{\mathrm{d}t}(x_i M) = \kappa_i^* x_i \tag{5.23}$$

where A_t is the bed cross-sectional area, M is the mass of particles in the bed and κ_i^* is the elutriation rate constant with units $kg/m^2 s$. From Eq. 5.23:

$$x_i = x_{i0} \exp\left(-\frac{\kappa_i^* A_t t}{M}\right) \tag{5.24}$$

where x_{i0} is the initial mass fraction of the particles at time zero. There are many empirical correlations for κ_i^* in terms of the physical properties of gas and particles (Kunii and Levenspiel 1991) from which it is clear that the particle terminal-fall velocity, u_t, is an important factor and that the rate coefficient increases as u_t decreases. Increasing pressure would thus be expected to increase the rate of elutriation, a result confirmed by Chan and Knowlton (1984) in a study of a bed of sand particles with a wide size distribution at pressures of up to 31 bar (Fig. 5.11)
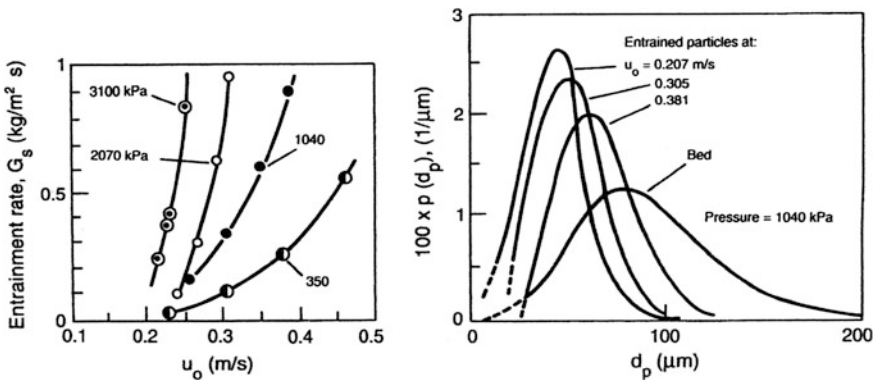

Fig. 5.11 Effect of pressure and fluidizing gas velocity on solids entrainment (Kunii and Levenspiel (1991) based on data of Chan and Knowlton (1984)

5.4.5   Heat Transfer

Fluidized-bed heat transfer is a major consideration in the design of reactors particularly those involving exothermic reactions. The field is very wide and has been reviewed in depth in a number of studies over the years a recent comprehensive example being that by Chen (2003) who pointed out that the mechanisms of transfer are significantly different for different fluidization regimes the two most important for industrial applications being bubbling beds and fast, circulating beds. Grace (1986) produced a "fluidization map" (Fig. 5.12) in which the various flow regimes are plotted as functions of a dimensionless particle diameter, d_p^*, and a dimensionless velocity, u^* where:

$$d_p^* = d_p \left[\frac{\rho_g (\rho_p - \rho_g) g}{\mu^2} \right]^{1/3} = Ar^{1/3} \tag{5.25}$$

Fig. 5.12 Regions of operation of fluidized beds of industrial significance (After Grace 1986)
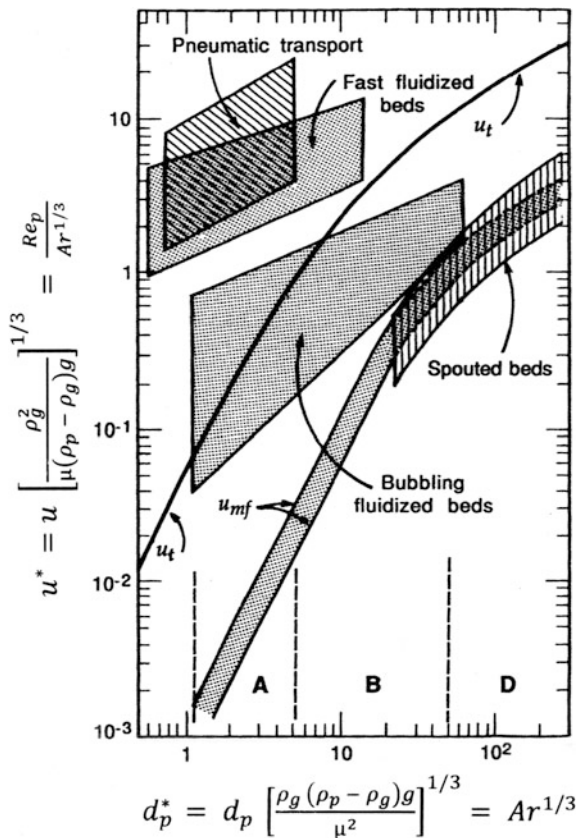
$$u^* = u \left[\frac{\rho_g^2}{\mu(\rho_p - \rho_g)g} \right]^{1/3} = \frac{Re_p}{Ar^{1/3}} \qquad (5.26)$$

Incorporating the physical properties of particles and gas with values of fluidizing gas velocities thus enables the operating regime to be identified; most industrial reactors operate within the regions indicated on the map. Some of these applications involve operation at elevated pressures and it is important to appreciate how the transfer process changes from ambient as pressure is increased (Fig. 5.12).

5.4.5.1   Bubbling Beds

As a result of the high surface area available in the particulate phase heat transfer between fluidizing gas and bed particles is normally very efficient and will not be considered further here although it is treated in some detail in Chen (2003). It is generally accepted that the heat transfer coefficient between a bed and an immersed surface can be expressed as the sum of three components:

$$h = h_{pc} + h_{gc} + h_r \qquad (5.27)$$

where h_{pc}, h_{gc} and h_r are the particle convective, gas convective and radiative transfer coefficients respectively. The gas convective term is of importance only for beds of large Group B and Group D materials while the radiative component is of significance only above about 600 °C so that for Group A and small Group B materials in the absence of radiation effects it is h_{pc} that dominates the heat transfer process. Several different approaches have been employed to estimate values of h_{pc}. Early work by Leva et al. (1949) on vertical surfaces proposed the following correlation for the heat-transfer Nusselt number in terms of k_g, the thermal conductivity of the fluidizing gas and Re_p the particle Reynolds number:

$$Nu_{pc} = \frac{h_{pc}d_p}{k_g} = 0.525 \left(Re_p\right)^{0.75} \qquad (5.28)$$

Similar correlations were proposed by Wender and Cooper (1958), Andeen and Glicksman (1976), Borodulya et al. (1991) and Molerus et al. (1995). An alternative approach, the so-called "packet theory" was originated by Mickley and Fairbanks (1955) and pictured bed-to-surface heat transfer as an unsteady-state process in which packets of emulsion-phase material carry heat to or from the surface, residing there for a short period of time before moving back into the bulk of the bed and being replaced by fresh material. The model gives a value for the instantaneous heat-transfer coefficient, h_i, as:

$$h_i = \left[\left(\frac{k_{mf}\,\rho_{mf}C_{mf}}{\pi\tau}\right)\right]^{1/2} \tag{5.29}$$

where k_{mf}, ρ_{mf} and C_{mf} are the thermal conductivity, density and heat capacity of the emulsion phase respectively and τ is the residence time of the packet at the wall. The effective conductivity of the emulsion phase may be given by:

$$k_{mf} = k_e^0 + 0.1\rho_g C_g d_p u_{mf} \tag{5.30}$$

k_e^0 being the conductivity of a fixed bed containing a stagnant gas. The main effect of increasing pressure will be to raise the gas density which will affect Re_p but have only a slight effect on h_{pc} through its influence on k_{mf}. For Group A and small Group B particles the suppression of bubbling caused by increasing pressure will increase the heat transfer by improving the quality of fluidization near the transfer surface as reported by Borodulya et al. (1982) who found an increase of 30 % in the maximum heat transfer coefficient for 0.126 mm sand particles between 6 and 81 bar. For larger particles the effect of pressure is to increase the gas-convective component via the increase in Re_{mf}. These trends have been confirmed by the work of Botterill and Desai (1972), Botterill and Denloye (1978), Staub and Canada (1987), Canada and McLaughlin (1978), Xavier et al. (1980) and Olsson and Almstedt (1995).

5.4.5.2 Circulating Beds

Owing to the danger of tube erosion caused by fast-moving solid particles heat exchange is normally carried out via cooling/heating tubes mounted in the walls of the vessel rather than by tubes immersed in the bed. The bed-to-wall heat exchange coefficient, h_w, is given by:

$$h_w = \frac{q}{a_w(T_b - T_w)} \tag{5.31}$$

where q is the rate of heat transfer, a_w is the area of exposed surface and T_b and T_w are the temperatures of bed and wall respectively. The many experimental measurements carried out to determine values of h_w have been reviewed by Chen (2003) who summarized the main observations to include:

- h_w is higher than that for gas convection at the same velocity but lower than that for bubbling beds
- h_w decreases with increasing particle size
- h_w increases with increasing solids mass flux
- h_w decreases with increasing height in the bed

There are many different correlations for h_w in the literature but no one is generally applicable and they will not be reviewed here—again the interested reader is referred to Chen (2003) for a comprehensive survey. One example will be given to illustrate the general approach. Werdermann and Werther (1993) proposed the following correlation for the particle-convective component of h_w for vertical surfaces in excess of 0.5 m in length in a CFB:

$$\frac{h_{pc}d_p}{k_g} = 7.46 \times 10^{-4} \left(\frac{D\rho_g U_g}{\mu_g}\right)^{0.757} \left(\frac{\rho_b}{\rho_p}\right)^{0.502}. \tag{5.32}$$

where D is the diameter of the column, U_g is the superficial gas velocity and ρ_b is the cross-sectional-average bed density (Grace and Bi 2003).

For circulating beds operated at high temperatures such as combustors the radiative component of h_w must be taken into account since these have been found to increase linearly with temperature to contribute over 35 % of the total at temperatures above 800°C (Ozkaynak et al. 1983). There are as yet few reports of heat-transfer measurements in circulating pressurized fluidized beds although their hydrodynamics have been studied in a number of cases. Thus Karri and Knowlton (1997) showed that solids hold-up decreased at pressures of 6.9 bar while Wirth and Gruber (1997) found solids to be more uniformly distributed over the full height of a CFB riser ay pressures of up to 50 bar (Grace and Bi 2003). Both effects would be expected to influence the heat-transfer performance of such units.

5.5 Conclusions

This chapter has demonstrated the important role that process conditions, namely temperature and pressure, play on the fluidization behavior of gas solid fluidized beds. Prediction of the fluidization behavior at process conditions is of major importance given that most of the industrial processes which use fluidized beds are operated at temperatures and pressures well above ambient. This chapter has explored the complexity of accounting for both hydrodynamic and interparticle effects with increasing temperature. It has also reviewed the effect of pressure on key design parameters such as entrainment, heat transfer and jet penetration. Although achieving a full understanding of the effect of process conditions on fluidization still remains a challenge, the theories and models presented in this chapter and developed over the last few decades have contributed to a key advancement in fluidized-bed design and operations.

References

Abrahamsen A, Geldart D (1980) Behaviour of gas-fluidized beds of fine powders part II. Voidage of the dense phase in bubbling beds. Powder Technol 26:47–55

Andeen BR, Glicksman LR (1976) Heat transfer to horizontal tube in shallow fluidized beds. Nat Heat Transfer Conf, St Louis MO, Paper 76-HT-67

Avidan AA, Yerushalmi J (1982) Bed expansion in high velocity fluidization. Powder Technol 32:223–232

Baerns M (1966) Effect of interparticle adhesive forces on fluidization of fine particles. Ind Eng Chem Fund 5(4):508–516

Boland D, Geldart D (1971) Electrostatic Charging in gas fluidized beds. Powder Technol 5:289–297

Borodulya VA, Epanov YG, Teplitskii YS (1982) Fluidized bed heat transfer. J Eng Phys 42:528

Borodulya VA, Teplitsky YS, Sorokin AP, Markevitch IL, Hassan AF, Yeromenko TP (1991) Heat transfer between a surface and a fluidized bed: considerations of temperature and pressure effects. Int J Heat Mass Transfer 34:47–53

Botterill JSM, Denloye AOO (1978) Ber-to-surface heat transfer in fluidized beds of large particles. Powder Tech 19:197–203

Botterill JSM, Desai M (1972) Limiting factors in gas-fluidized bed heat transfer. Powder Tech 6:231–238

Botterill JSM, Teoman Y, Yüregir KR (1982) The effect of operating temperature on the velocity of minimum fluidization, bed voidage and general behaviour. Powder Technol 31:101–110

Broadhurst TE, Becker HA (1975) Onset of fluidization and slugging in beds of uniform particles. AIChE J 21:238–247

Bruni G, Lettieri P, Newton D, Yates JG (2006) The influence of fines size distribution on the behaviour of gas fluidized beds at high temperature. Powder Technol 163:88–97

Canada GS, MacLaughlin MH (1978) Large-particle fluidization and heat transfer at high pressure. AIChE Symp Ser 74(176):27–37

Carman PC (1937) Fluid flow through granular beds. Trans Inst Chem Eng 15:150

Castellanos A (2005) The relationship between attractive interparticle forces and bulk behaviour in dry and uncharged fine powders. Adv Phys 54:263–376

Chan IH, Knowlton TM (1984) The effect of pressure on entrainment from bubbling gas-fluidized beds. In: Kunii D, Toei R (eds) Fluidization. Engineering Foundation, New York, pp 283–290

Chen JC (2003) Heat transfer. In: Yang W-C (ed) Handbook of fluidization and fluid-particle systems (Chapter 3). Marcel Dekker, New York

Chen ZD, Chen XP, Wu Y, Chen RC (2010) Study on minimum fluidization velocity at elevated temperature. Proc Chin Soc Electr Eng 30:21–25

Clift R, Grace JR, Weber ME (1974) Stability of bubbling fluidized beds. I E C Fundam 13:45–51

Compo P, Pfeffer R, Tardos GI (1987) Minimum sintering temperature and defluidization characteristics of fluidizable materials. Powder Technol 51:85–101

D'Amore M, Donsi' G, Massimilla L (1979) The influence of bed moisture on fluidization characteristics of fine powders. Powder Technol 23:253–259

Davidson JF, Harrison D (1963) Fluidized particles. Cambridge University Press, Cambridge

Doichev K, Akhmakov N (1979) Fluidisation of polydisperse systems. Chem Eng Sci 2–4

Donsì G, Massimilla L (1973). Bubble-free expansion of gas-fluidized beds of fine particles. AIChE J 19:1104–1110

Ennis BJ, Tardos G, Pfeffer R (1991) A microlevel-based characterisation of granulation phenomena. Powder Technol 65:257–272

Ergun S (1952) Fluid flow through packed columns. Chem Eng Prog 48(2):89–94

Fairbrother R (1999) A microscopic investigation of particle-particle interactions in the presence of liquid binders in relation to the mechanisms of "wet" agglomeration processes. PhD Dissertation, Department of Chemical Engineering, University College London

Formisani B, Girimonte R, Mancuso L (1998) Analysis of the fluidization process of particle beds at high temperature. Chem Eng Sci 53:951–961

Foscolo PU, Gibilaro LG (1984) A fully predictive criterion for the transition between particulate and aggregate fluidization. Chem Eng Sci 39(12):1667–1675

Foscolo PU, Gibilaro L (1987) Fluid dynamic stability of fluidised suspensions: the particle bed model. Chem Eng Sci 42(6):1489–1500

Geldart D, Wong ACY (1984) Fluidization of powders showing degrees of cohesiveness-I. Bed expansion. Chem Eng Sci 39(10):1481–1488

Geldart D, Wong ACY (1985) Fluidization of powders showing degrees of cohesiveness-II. Experiments on rates of de-aeration. Chem Eng Sci 40(4):653–661

Girimonte R, Formisani B (2009) The minimum bubbling velocity of fluidized beds operating at high temperature. Powder Technol 189:74–81

Girimonte R, Formisani B (2014) Effects of operating temperature on the bubble phase properties in fluidized beds of FCC particles. Powder Technol 262:14–21

Godard KMS, Richardson JF (1968) The behaviour of bubble-free fluidised beds. Inst Chem Eng Symp Ser 30:126–135

Goo JH, Seo MW, Kim SD, Song BH (2010) Effects of temperature and particle size on minimum fluidization and transport velocities in a dual fluidized bed. In: Proceedings of the 20th international conference on fluidized bed combustion. pp 305–310

Goroshko VD, Rozembaum RB, Toedes OH (1958) Approximate relationships for suspended beds and hindered fall. Izv Vuzov Neft Gaz 1:125

Grace JR (1986) Contacting modes and behaviour classification of gas-solid and other two-phase suspensions. Can J Chem Eng 64:353–363

Grace JR, Bi H (2003) Circulating fluidized beds. In: Yang W-C (ed) Handbook of fluidization and fluid-particle systems (Chapter 19). Marcel Dekker, New York

Grace JR, Lim CJ (1987) Permanent jet formation in beds of particulate solids. Can J Chem Eng 65(1):160–162

Grace JR, Sun G (1991) Influence of particle size distribution on the performance of fluidized bed reactors. Can J Chem Eng 69(5):1126–1134

Haider A, Levenspiel O (1989) Drag coefficient and terminal velocity of spherical and non-spherical particles. Powder Tech 58:63–70

Hamaker HC (1937) The London-Van der Waals attraction between spherical particles. Physica IV 10:1059–1068

Hartman M, Trnka O, Pohořelý M (2007) Minimum and terminal velocities in fluidization of particulate ceramsite at ambient and elevated temperature. Ind Eng Chem Res 46:7260–7266

Hirsan I, Shistla C, Knowlton TM (1980) The effect of bed and jet parameters on vertical jet penetration length in gas-fluidized beds. In: 73rd annual AIChE meeting, Chicago, Illinois

Hoffmann AC, Yates JG (1986) Experimental observations of fluidized beds at elevated pressures. Chem Eng Commun 41:133

Israelachvili J (1991) Intermolecular and surface forces. Academic Press, London

Jiliang M, Xiaoping C, Daoyin L (2013) Minimum fluidization velocity of particles with wide size distribution at high temperatures. Powder Technol 235:271–278

Karri SBR, Knowlton TM (1997) The effect of pressure on CFB riser hydrodynamics. In: Kwauk M, Li J (Eds) Circulating fluidized bed technology. Beijing Science Press, Beijing, pp 103–109

King DF, Harrison D (1980) The bubble phase in high-pressure fluidized beds. Grace JR, Matsen JM (eds) Fluidization. Plenum Press, New York, pp 101–107

King DH, Harrison D (1982) The dense phase of a fluidized bed at elevated pressures. Trans Inst Chem Eng 60:26–30

Knowlton TM (1992) Pressure and temperature effects in fluid-particle systems. Fluidization VII. Engineering Foundation, New York, pp 27–46

Kunii D, Levenspiel O (1991) Fluidization engineering. Butterworths, Boston

Landi G, Barletta D, Poletto M (2011) Modelling and experiments on the effect of air humidity on the flow properties of glass powders. Powder Technol 207:437–443

Landi G, Barletta D, Lettieri P, Poletto M (2012) Flow properties of moisturized powders in a Couette fluidized bed rheometer. Int J Chem Reactor Eng 10(A28):1–13

Lettieri P (1999) A study on the influence of temperature on the flow behaviour of solid materials in a gas fluidized bed. PhD thesis, University College, London

Lettieri P, Yates JG, Newton D (2000) The influence of interparticle forces on the fluidization behaviour of some industrial materials at high temperature. Powder Technol 110:117–127

Lettieri P, Newton D, Yates JG (2001a) High temperature effects on the dense phase properties of gas fluidized beds. Powder Technol 120:34–40

Lettieri P, Brandani S, Newton D, Yates JG (2001b) A generalization of the Foscolo and Gibilaro particle-bed model particle to predict the fluid stability of some fresh FCC catalysts at elevated temperatures. Chem Eng Sci 56(18):5401–5412

Leva M (1959) Fluidization. McGraw-Hill, New York

Leva M, Weintraub M, Grummer M (1949) Heat transmission through fluidized beds of fine particles. Chem Eng Prog 45:563–572

Leva M, Shirai T, Wen CY (1956) Prediction of onset of fluidization in beds of granular solids. Genie Chim 75:33

Lin C-L, Wey M-Y, You S-D (2002) The effect of particle size distribution on minimum fluidization velocity at high temperature. Powder Technol 126:297–301

Lucas A, Arnaldos J, Casal J, Puigjaner L (1986) High temperature incipient fluidization in mono and polydisperse systems. Chem Eng Commun 41:121–132

Massimilla L, Donsi' G (1976) Cohesive forces between particles of fluid-bed catalysts. Powder Technol 15(2):253–260

Massimilla L, Donsi' G, Zucchini C (1972) The structure of bubble-free gas fluidized beds of fine fluid cracking catalyst particles. Chem Eng Sci 27:2005–2015

Mickley HS, Fairbanks DF (1955) Mechanism of heat transfer to fluidized beds. AIChE J 1:374–384

Miller C, Logwinuk A (1951) Fluidization studies of solid particles. Ind Eng Chem 43:1220–1226

Molerus O, Burschka A, Dietz S (1995) Particle migration at solid surfaces and heat transfer in bubbling fluidized beds II. Prediction of heat transfer in bubbling fluidized beds. Chem Eng Sci 50:879–885

Mutsers SMP, Rietema K (1977) The effect of interparticle forces on the expansion of a homogeneous gas-fluidized bed. Powder Technol 18:239–248

Newton D, Smith G, Hird N (1996) Assessment of FCC catalysts evaluation criteria. In: Presented at the fourth international conference on fluid particle interaction, Davos, Switzerland

Olowson PA, Almstedt AE (1990) Influence of pressure and fluidization velocity on the bubble behaviour and gas-flow distribution in a fluidized bed. Chem Eng Sci 45:1733–1741

Olowson PA, Almstedt AE (1991) Influence of pressure on the minimum fluidization velocity. Chem Eng Sci 46:637–640

Olsson SE, Almstedt AE (1995) Local instantaneous and time-averaged het transfer in a pressurized fluidized bed with horizontal tubes: influence of pressure, fluidization velocity and tube-bank geometry. Chem Eng Sci 50:3231–3245

Ozkaynak TF, Chen JC, Frankenfield TR (1983) An experimental investigation of radiant heat transfer in high-temperature fluidized bed. In: Fluidization. Engineering Foundation, New York, Vol V, pp 371–378

Raso G, D'Amore M, Formisani B, Lignola PG (1992) The influence of temperature on the properties of the particulate phase at incipient fluidization. Powder Technol 72:71–76

Riba JP, Routie R, Couderc JP (1978) Conditions minimales de miseenfluidisation par unliquide. Can J Chem Eng 56:26–30

Richardson J, Zaki WN (1954) Sedimentation and fluidisation: Part I. Trans Inst Chem Eng 32:35–53

Rietema K, Piepers HW (1990) Effect of interparticle forces on the stability of gas-fluidized beds-I. Experimental evidence. Chem Eng Sci 45(6):1627–1639

Rietema K, Cottaar EJE, Piepers HW (1993) Effect of interparticle forces on the stability of gas-fluidized beds—II. Theoretical derivation of bed elasticity on the basis of van der Waals forces between powder particles. Chem Eng Sci 48(9):1687–1697

Rowe PN (1984) The effect of pressure on minimum fluidization velocity. Chem Eng Sci 39:173–174

Rowe PN, Santoro L, Yates JG (1978) The division of gas between bubble and interstitial phases in fluidized beds of fine powders. Chem Eng Sci 33:133–140

Seville JPK, Clift R (1984) The effect of thin liquid layers on fluidization characteristics. Powder Technol 37:117–129

Seville JPK, Silomon-Pflug H, Knight PC (1998) Modelling of sintering in high temperature gas fluidization. Powder Technol 97(2):160–169

Siegell JH (1984) High-temperature defluidization. Powder Technol 38:13–22

Siegell JH (1989) Early studies of magnetized fluidized beds. Powder Technol 57:213–220

Simons SJR, Seville JPK, Adams MJ (1993) Mechanisms of agglomeration. In: Sixth international symposium on agglomeration, Nagoya, Japan

Staub FW, Canada GS (1987) Effect of tube bank and gas density on flow behaviour and heat transfer in a fluidized bed. In: Davidson JF, Kearns DL (eds) Fluidization. Cambridge University Press, Cambridge, pp 339–344

Subramani HJ, MothivelBalaiyya MB, Miranda LR (2007) Minimum fluidization velocity at elevated temperatures for Geldart's group-B powders. Exp Therm Fluid Sci 32:166–173

Tardos G, Mazzone D, Pfeffer R (1985) Destabilization of fluidized beds due to agglomeration, Part I: Theoretical model. Can J Chem Eng 63:377–383

Valverde JM, Castellanos A (2008) Bubbling suppression in fluidized beds of fine and ultrafine powders. Part Sci Technol 26:197–213

Valverde JM, Quintanilla M, Castellanos A, Mills P (2001) The settling of fine cohesive powders. Europhys Lett 54:329–334

Valverde JM, Castellanos A, Mills P, Quintanilla M (2003) Effect of particle size and interparticle force on the fluidization behavior of gas-fluidized beds. Phys Rev E Stat Nonlin Soft Matter Phys 67:051305

Wen CY, Yu YH (1966) Mechanics of fluidization. Chem Eng Progr Symp Ser 62:100–111

Wender L, Cooper GT (1958) Heat transfer between fluidized-solids bed and boundary surfaces—correlation of data. AIChE J 4:15–23

Werdermann CC, Werther J (1993) Solids flow pattern and heat transfer in an industrial-scale fluidized-bed heat exchanger. In: Proceedings of 12th international conference on fluid-bed combustion, vol 2, pp 985–990

Wirth KE, Gruber U (1997) Fluid mechanics of circulating fluidized beds with small-density ratio of solids to fluid. In: Kwauk M, Li J (eds) Circulating fluidized-bed technology. Beijing Science Press, Beijing, pp 78–83

Wu S, Baeyens J (1991) Effect of operating temperature on minimum fluidization velocity. Powder Technol 67:217–220

Xavier AM, King DF, Davidson JF, Harrison D (1980) Surface-bed heat transfer in a fluidized bed at high pressure. In: Grace JR, Matsen JM (eds) Fluidization. Plenum, New York, pp 209–216

Xie HY, Geldart D (1995) Fluidization of FCC powders in the bubble-free regime: effect of types of gases and temperature. Powder Technol 82:269–277

Yamazaki R, Han NS, Sun ZF, Jimbo G (1995) Effect of chemisorbed water on bed voidage of high temperature fluidized bed. Powder Technol 84:15–22

Yang W-C (1981) Jet penetration in a pressurized fluidized bed. I E C Fundam 20:297–300

Yates JG (1996) Effects of temperature and pressure on gas fluidization. Chem Eng Sci 51: 167–205

Yates JG (2003) Effect of temperature and pressure. In: Yang W-C (ed) Handbook of fluidization and fluid-particle systems (Chapter 5). Marcel Dekker, New York

Yates JG, Bejcek V, Cheesman DJ (1986) Jet penetration into fluidized beds at elevated pressures. In: Ostergaard K, Sorensen S (eds) Fluidization V. Engineering Foundation, New York, pp 79–86